Dual control of active graphene–silicon hybrid metamaterial devices

Li, Quan; Tian, Zhen; Zhang, Xueqian; Xu, Ningning; Singh, Ranjan; Gu, Jianqiang; Lv, Peng; Luo, Lin-bao; Zhang, Shuang; Han, Jiaguang; Zhang, Weili

DOI:
10.1016/j.carbon.2015.04.015

License:
Other (please specify with Rights Statement)

Document Version
Peer reviewed version

Citation for published version (Harvard):
Li, Q, Tian, Z, Zhang, X, Xu, N, Singh, R, Gu, J, Lv, P, Luo, L, Zhang, S, Han, J & Zhang, W 2015, 'Dual control of active graphene–silicon hybrid metamaterial devices', Carbon, vol. 90, pp. 146-153. https://doi.org/10.1016/j.carbon.2015.04.015

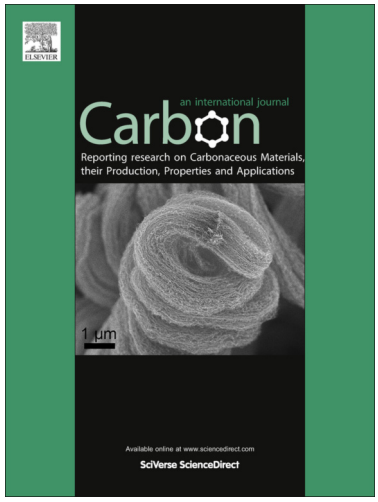

Dual control of active graphene-silicon hybrid metamaterial devices

Quan Li, Zhen Tian, Xueqian Zhang, Ningning Xu, Ranjan Singh, Jianqiang Gu, Peng Lv, Lin-Bao Luo, Shuang Zhang, Jiaguang Han, Weili Zhang

PII: S0008-6223(15)00295-X
DOI: http://dx.doi.org/10.1016/j.carbon.2015.04.015
Reference: CARBON 9833

To appear in: *Carbon*

Received Date: 3 December 2014
Accepted Date: 6 April 2015

Please cite this article as: Li, Q., Tian, Z., Zhang, X., Xu, N., Singh, R., Gu, J., Lv, P., Luo, L-B., Zhang, S., Han, J., Zhang, W., Dual control of active graphene-silicon hybrid metamaterial devices, *Carbon* (2015), doi: http://dx.doi.org/10.1016/j.carbon.2015.04.015

Dual control of active graphene-silicon hybrid metamaterial devices

Quan Li [a,†], Zhen Tian [a,*,†], Xueqian Zhang [a], Ningning Xu [b], Ranjan Singh [c], Jianqiang Gu [a], Peng Lv [d], Lin-Bao Luo [d], Shuang Zhang [e], Jiaguang Han [a,*], Weili Zhang [a,b,*]

[a] Center for Terahertz waves and College of Precision Instrument and Optoelectronics Engineering,
Tianjin University and the Key Laboratory of Optoelectronics Information and Technology (Ministry of Education), Tianjin 300072, China.

[b] School of Electrical and Computer Engineering, Oklahoma State University, Stillwater, Oklahoma 74078, USA.

[c] Center for Disruptive Photonic Technologies, Division of Physics and Applied Physics, School of Physical and Mathematical Sciences, Nanyang Technological University, 21 Nanyang Link, Singapore 637371

[d] School of Electronic Science and Applied Physics, Hefei University of Technology, Hefei, Anhui 230009, China.

[e] School of Physics and Astronomy, University of Birmingham, Birmingham B15 2TT, UK.

[†]These authors equally contributed to this work

*email: tianzhen@tju.edu.cn; jiaghan@tju.edu.cn; weili.zhang@okstate.edu

Abstract

Metamaterials offer enormous opportunities and unprecedented functionalities to manipulate electromagnetic waves enabling promising applications such as invisibility cloaking, superfocusing and subwavelength confinement. The exotic electromagnetic behavior of metamaterials was dramatically empowered by dynamic control through incorporation of active media. A prominent example is a graphene metamaterial-an integration of a two-dimensional monolayer graphene with a planar metasurface, where the unique optical and electronic properties of graphene is inherited by the metamaterial, thus opening up fascinating possibilities in

electromagnetic wave control. Here, through a combination of continuous wave (CW) optical illumination and electrical gating, we demonstrate a giant active modulation of terahertz waves in a graphene-silicon hybrid metamaterial at extremely low bias voltages. The highly tunable characteristics of the graphene metamaterial device under electrical bias and optical illumination open up new avenues for graphene-based high performance integrated active photonic devices compatible with the silicon technology.

1. Introduction

Advances in metamaterials which possess unusual and exotic electromagnetic properties hold the promise to enable technological breakthroughs in controlling radiation at microwave, terahertz, infrared and optical frequencies [1-11]. In the terahertz regime, various metamaterial-based devices including filters [12], modulators [13], switches [14,15], and invisibility cloaks [16-18] have been well demonstrated. The flexibilities to design and engineer metamaterials at will are opening up application opportunities in non-invasive testing, sensing, security screening, and telecommunications, thus hastening the advancement of the technologically important terahertz domain. The impact of such subwavelength devices would be tremendously enhanced if the resonance response characteristics of metamaterials could be dynamically tuned. Therefore, continued interest in terahertz metamaterials highly depends on the discovery of novel devices with real time modulation. Efforts underway in several groups led to the demonstration of active

manipulation of terahertz waves by applying electrical control [4,19], magnetostatic control [20], and optical illumination [21-23]. The dynamic control was initially introduced in metamaterial-semiconductor hybrid structures and their terahertz responses were tuned by external stimulus that modified the carrier dynamics of the semiconductor inclusions.

Recently, graphene has emerged as a new material in the field of material science and condensed matter physics due to its ultra-high quality, stable monolayer crystalline structure, and unusual electrical properties [24]. As a single layer of strictly two-dimensional carbon atoms, graphene also possesses unique mechanical, optical, thermal, and magnetic properties with a plethora of exciting applications that are being pursued vigorously. To date, various approaches including chemical functionalization, surface modification, and impurity atom doping have been developed to tailor the electrical and optical properties of graphene [25-30], which renders it to be an extremely attractive candidate for a favorable active ingredient in metamaterial design, particularly at the terahertz regime. Recently, tunable terahertz response was successfully realized in an engineered graphene microribbon metamaterial by electrostatic doping [31]. A terahertz gate-controlled modulator consisting of a graphene metamaterial was also demonstrated with a high external gate voltage of 850 V [5]. In addition, with a low gate bias of 0.5 V, maximum modulation of 18% was achieved in a split-ring resonator (SRR)-based graphene metamaterial [9]. The underlying mechanism is that the gate voltage allows the tuning

of the Fermi level and the corresponding charge carrier density of the integrated graphene layer.

In this article, we demonstrate a giant modulation of terahertz response in a highly efficient, dual-control graphene-silicon hybrid metasurface device. Unlike in the previous works where a thick oxide layer was sandwiched between the graphene and silicon substrate that shares a large fraction of the voltage drop applied at the gate [27,32], here the graphene is directly transferred onto the silicon substrate. Under optical illumination, the photo-carriers generated in silicon directly diffuse into graphene, thus allowing for a highly efficient tuning of the Fermi level in the graphene film. As such, a small gate voltage would dramatically change the graphene conductivity and consequently modulate the terahertz response in the hybrid metamaterial. This particular scheme would tremendously expand the scope of novel and compact graphene-based terahertz photonic devices.

2. Experimental details

2.1 Design of the graphene metamaterials

The hybrid graphene metasurface modulator is illustrated in Fig. 1. The two-dimensional metasurface, consisting of 200-nm-thick aluminum SRRs, was lithographically fabricated on a 630-μm-thick *p*-type silicon wafer. Here, the aluminum thickness of 200-nm was chosen to ensure the optimized resonance behavior of the SRRs [33], while the dimensions of the SRRs were determined to resonate at terahertz frequencies [4,34,35]. A large-area monolayer graphene grown

by copper-catalyzed chemical vapor deposition (CVD) was then transferred onto the planar metasurface [36-38]. The corresponding Raman spectrum is shown in Fig. S1 in the Supporting Information to identify the quality of the graphene monolayer. In order to tune the conductivity of graphene and allow for a large transmission of the incident terahertz beam, a square-ring electrode was carefully designed and incorporated onto the top and bottom surface of the hybrid metamaterial, as illustrated in Fig. 1(a).

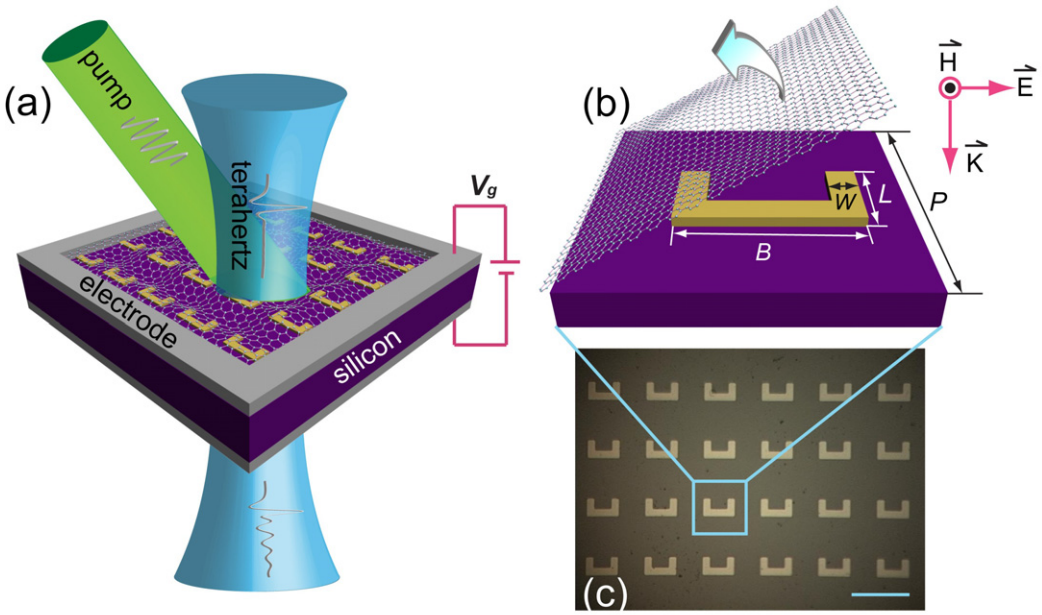

Fig. 1 - (a) Monolayer graphene deposited on the SRRs with continuous wave laser light excitation and applied bias voltage V_g. (b) Schematic of the unit structure with parameters: P = 100 μm, W = 12 μm, L = 30 μm, B = 54 μm. (c) Microscopic image of the fabricated graphene-silicon hybrid metamaterial. Scale bar, 100 μm.

2.2 Characterization of the graphene metamaterials

The metamaterial samples were characterized by broadband terahertz time-domain spectroscopy (THz-TDS) [39]. An 8-F confocal THz-TDS system focused the beam to a 3.5 mm diameter waist and was collimated on the gate-controlled active metamaterial. An optical pump beam (CW laser beam at 532 nm) with a spot diameter of ~6 mm enabled a uniform excitation of the samples. All measurements were carried out at room temperature in a dry air environment to eliminate the absorption of terahertz waves by water vapor present in the atmosphere. As shown in Fig. 1(b), the incident electric field polarization was kept parallel to the gap of the U-shaped SRR to excite the inductive-capacitive (LC) resonance [40]. The transmission spectrum was extracted as $\tilde{t}(\omega) = \tilde{E}_s(\omega)/\tilde{E}_r(\omega)$, where $\tilde{E}_s(\omega)$ and $\tilde{E}_r(\omega)$ are the measured transmission of the sample and the reference (a bare-silicon substrate without photoexcitation and gate bias), respectively [21,35].

3. Results and discussion

3.1 Functionality and operation

Fig. 2(a) shows the measured amplitude transmission $|\tilde{t}(\omega)|$ through the graphene metamaterial with different applied gate bias voltage V_g under 280 mW optical excitation. Without photoexcitation and at zero gate voltage, a pronounced LC resonance approximately at 0.67 THz is observed irrespective of the presence or absence of the graphene layer (Fig. S2, in Supporting Information). The resonance frequency is determined by $f_0 = 1/2\pi\sqrt{LC}$ where the inductance (L) and capacitance (C) plays a dominant role [14]. The LC resonance line width is limited by the

effective resistance (R) in the SRRs. When optical illumination is applied and a positive gate voltage (Fig. 1(a)) V_g is increased from 0 to 5 V, the terahertz transmission is enhanced, peaking at V_g = 1 V (Fig. 2(b)) where the Fermi level of graphene is much closer to the Dirac point [41]. At V_g = 1 V, the measured amplitude modulation depth $\left|(T_{V_g} - T_{V_0})/T_{V_0}\right|$ reaches ~61% at the resonance frequency, where T_{V_0} and T_{Vg} are the transmission amplitudes for zero and V_g gate voltages, respectively. With further increase in V_g, however, we observed a reversal of the increasing transmission trend. Thus, with V_g = 5 V, the resonance dip as low as 0.38 is observed in the transmission spectrum. On the other hand, when a negative voltage V_g is applied, the transmission decreased dramatically. As shown in Fig. 2(a), when V_g = -5 V, the LC resonance becomes weak and the resonance dip decreased significantly to 0.17 with a modulation depth approaching ~39%. The voltage dependent transmission at the dip of LC resonance is summarized in Fig. 2(b).

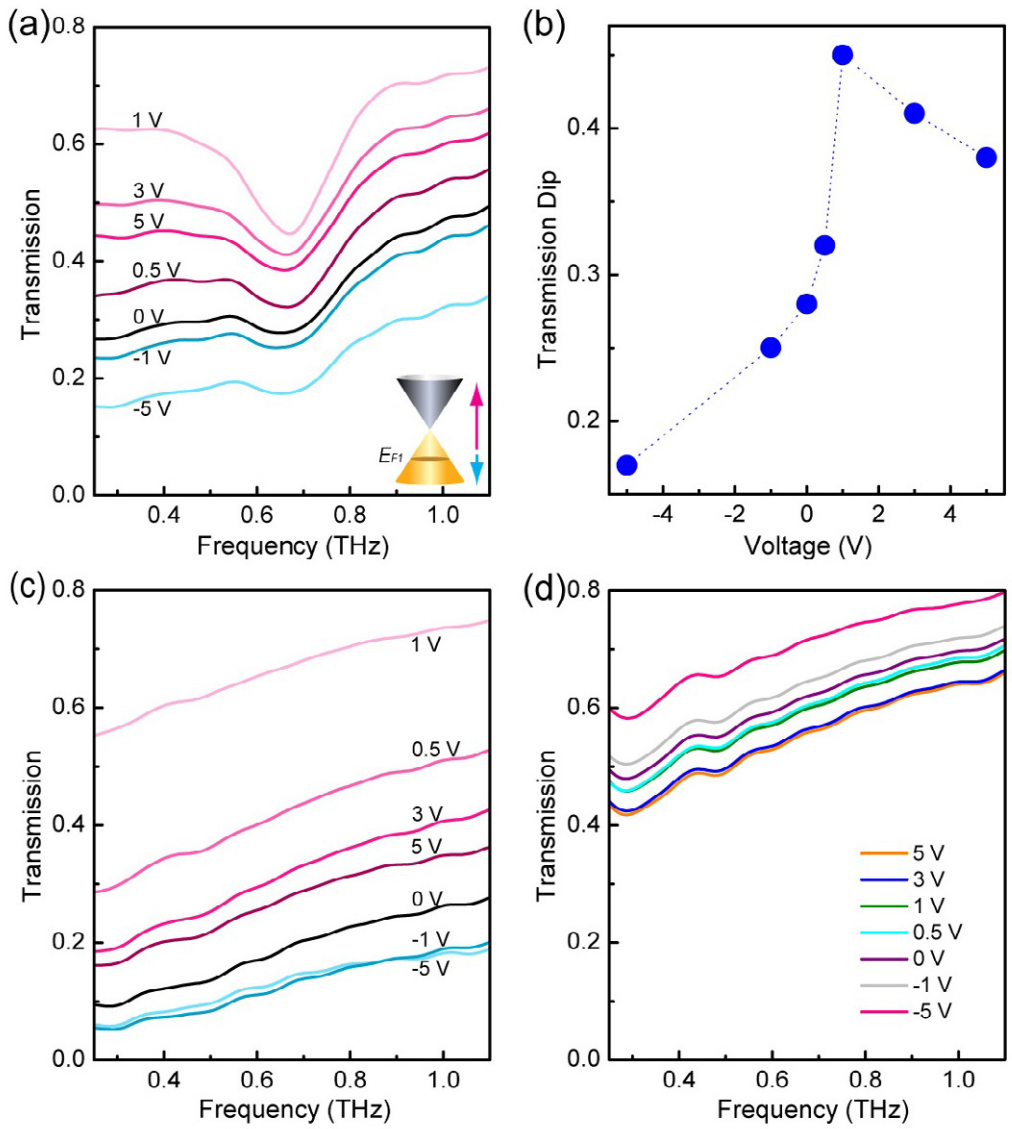

Fig. 2 - (a) Measured transmission amplitude of the graphene metamaterial as a function of frequency at various gate biases under 532 nm, 280 mW light illumination. (b) Voltage-dependent transmission amplitude at the dip position of the LC resonance corresponding to (a). (c) Measured transmission amplitude of unpatterned monolayer graphene on silicon substrate as a function of frequency at various gate biases under 532 nm, 280 mW light illumination. (d) The measured transmission amplitude of the bare silicon as a function of frequency at various gate biases under 532 nm, 280 mW

light illumination. Inset of (a): Schematic diagram of the Fermi level, corresponding to (a).

3.2 Effect of the graphene on the silicon substrate

The interesting characteristics observed in the active modulation of the LC resonance in the metamaterial were attributed mainly to the modification in the conductivity of graphene and a thin top layer of the silicon substrate with varying gate voltages under optical illumination. Due to limited penetration depth of the green light into silicon (~1 μm) [42], the substrate can be considered as a photodoping-dependent conductive thin silicon layer atop a lossless silicon bulk layer [43,44]. The schematic of the multistack system is shown in the inset of Fig. 3(a). In order to elucidate the modulation effect of graphene-silicon hybrid metamaterial in further detail, the transmission characteristics of the monolayer graphene on silicon (GOS) without SRRs were experimentally measured. Fig. 2(c) shows the measured transmission spectra through the GOS sample at different applied gate voltages V_g under 280 mW of continuous optical pump excitation. Without the SRR metallic units, the GOS showed a similar modulation performance at different voltages, where the transmission increased as the voltage gradually varied from -5 to 1 V but showed a decreasing trend as the bias voltage increased from 1 to 5 V. However, we noticed a dramatic increase in transmission when the voltage changed from 0 to 0.5 V and a minor variation from -1 to -5 V. Apparently, the effect of the voltage applied on GOS differed from that on the graphene-silicon hybrid metasurface due to absence of the

metallic SRR structures and the difference in the quality of graphene monolayer film that was deposited on both samples. Thus the transmission amplitude through the plain GOS only reveals a similar trend to that in the hybrid graphene-silicon metamaterial.

3.3 Effective conductivity

By applying standard thin-film approximation [28,45], we extracted the frequency-dependent complex effective conductivity $\tilde{c}_{eff}(\omega)$ of the hybrid graphene monolayer and photodoped silicon top layer (inset of Fig. 3(a)) from the measured terahertz transmission

$$\tilde{t}(\omega) = \frac{1}{1 + Z_0 \tilde{\sigma}_{eff}(\omega) d / (1 + n_s)} \quad , \tag{1}$$

where Z_0 is the impedance of free space; d is the total thickness of the graphene monolayer and the photodoped silicon layer, it is assumed to be 1 μm due a huge difference in the thickness of graphene (< 1 nm) and photodoped silicon layer (~1 μm); and n_s is the refractive index of the lossless silicon substrate.

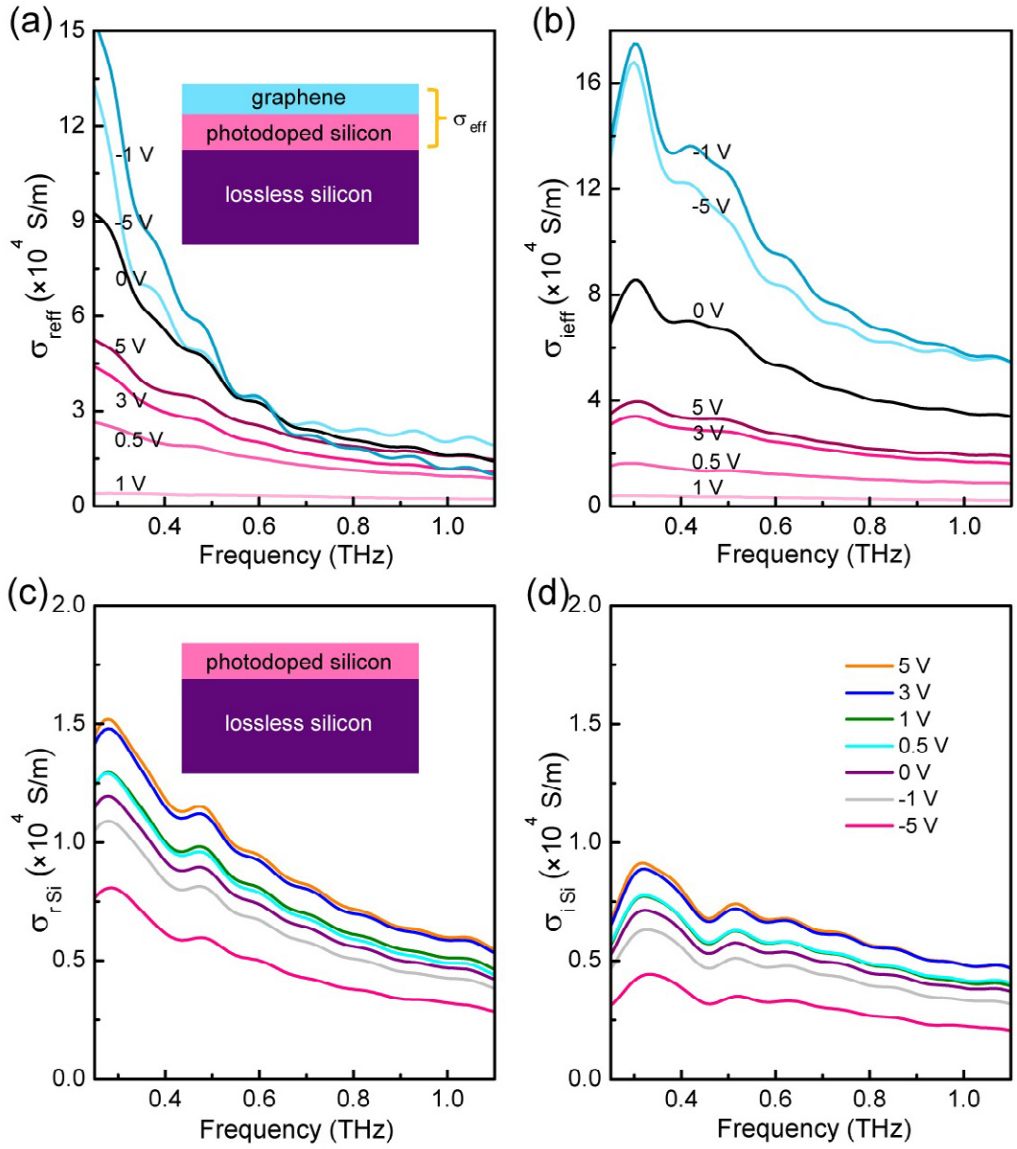

Fig. 3 - Extracted real (a) and imaginary (b) part of the effective conductivity. Extracted real (c) and imaginary (d) part of the conductivity of the photodoped top layer of the bare silicon at various gate biases under 532 nm, 280 mW light illumination (corresponding to Fig. 2(d)) using thin-film approximation. Insets: Schematics of the corresponding multistack systems.

As shown in Fig. 3(a) and (b), the real and imaginary part of the complex conductivity ($\tilde{c}_{eff}(a) = c_{reff} + ic_{ieff}$) of the effective layer for different gate voltage at

280 mW optical excitation has been extracted by inverting Eq. (1) with the measured complex transmission $\tilde{t}(\omega)$. The terahertz transmission decreased with increase in the real and imaginary part of conductivity of the GOS film. Therefore, the gate-controlled terahertz transmission through the metamaterial (Fig. 2(a)) is ascribed to the dynamic tuning of the effective conductivity of the graphene-silicon hybrid film (Fig. S4(a)). This can be understood as: i) the effective conductivity change cause the overall transmission modification; ii) the effective conducting layer behaves as a variable resistance which shorts the LC resonance at the gap, where the larger conductivity corresponds to increased free carries absorption at the resonance, resulting in decreased LC resonance strength and increased bandwidth [4]. Thus, both the modulation depth of the amplitude transmission and the device bandwidth of the resonance are limited by the maximum range the conductivity can be modified. Same trend of transmission change happens when using SRRs with different sizes or scales, in which the functioning resonance frequency would be different.

To gain further in-depth understanding of the transport properties in the graphene metamaterial, the frequency dependent effective conductivity can be expressed as $\tilde{c}_{eff}(\omega) = a\tilde{c}_{gr}(\omega) + b\tilde{c}_{Si}(\omega)$, where a and b are scaling factors, $\tilde{c}_{gr}(\omega)$ and $\tilde{c}_{Si}(\omega)$ are the respective conductivities of graphene and the photodoped silicon layer. For comparison these two parts of conductivities, the bare silicon tuned by various electrical voltages with optical illumination power of 280 mW was also characterized. As shown in Fig. 2(d), the transmission sees a moderate drop as the gate voltage varied from -5 to 5 volts, revealing only a subtle modulation (the highest modulation

depth at 0.67 THz equals to 16%). We must stress that the modulation mechanism in the bare silicon is different from that of the graphene metamaterial, leading to the distinct transmission variation trend. The corresponding real $\varepsilon_{rSi}(\omega)$ and imaginary $\varepsilon_{iSi}(\omega)$ part (Fig. 3(c) and (d)) of the photodoped top layer of the bare silicon (inset of Fig. 3(c)) is approximately an order of magnitude lower than that of the effective conductivity of graphene-silicon hybrid film (Fig. 3(a) and (b)). Thus it is justified to assume that the graphene conductivity component is larger than the silicon conductivity, and the observed transmission change in Fig. 2a mainly arises from the doping of the graphene layer. This could be due to the higher carrier mobility in graphene and can be expressed by the Kubo formula/Drude model which depends on the Fermi energy E_F and carrier scattering rate Γ [5,28]. Under a constant optical excitation, the carrier scattering rate does not change significantly with the gate voltage [41]. Therefore, irrespective of positive or negative sign of bias, $\tilde{\varepsilon}_{Si}(\omega)$ changes on a small scale with increasing gate voltage, while the dependence of $\tilde{\varepsilon}_{gr}(\omega)$ upon gate voltage is attributed to the modification of the energy band structure of graphene.

3.4 Modulation of Fermi energy

The graphene film examined here was prepared by use of chemical vapor deposition (CVD) processing and was *p*-type doped, whose Fermi energy, E_F, is near the Dirac point in the valence band [25]. With continuous optical excitation, large density of carriers (the density of holes N_h is greater than that of electrons N_e) were excited in

the photodoped silicon layer while the amount of electron-hole pairs generated in graphene was negligible [44,46]. Namely, the silicon layer illuminated by the CW laser serves as a rich source of carriers. The free carriers ($N_h > N_e$) diffuse from silicon into the graphene flake due to the charge gradient between their interface until an equilibrium is reached, leading to a larger gap between the original Fermi level E_{F1} (under illumination but without any bias voltage) and Dirac point (inset of Fig. 2(a)). The modulation process of the graphene monolayer differed significantly for positive and negative sign of the voltage bias: (i) When a positive bias is applied, the electrons from silicon drifted into the graphene flake. These electrons first recombine with holes in graphene altering the Fermi level that moves toward the Dirac point (as indicated by the pink arrow in the inset of Fig. 2(a)). As a result, the conductivity of graphene $\tilde{\sigma}_{gr}(\omega)$ as well as effective conductivity $\tilde{\sigma}_{eff}(\omega)$ decreased, thus enhancing the LC resonance of the metamaterial. The Fermi level initially moved closer and then farther from the Dirac point in the conduction band when the positive voltage continued to increase. This strengthened the metallic property of graphene and enhanced $\tilde{\sigma}_{eff}(\omega)$ that quenched the on-resonance transmission of the graphene-silicon hybrid metamaterial (pink curves of 1 to 5 V in Fig. 2(a)). (ii) When a negative bias is applied, the holes from silicon drifted into the graphene sheet. Therefore, the Fermi level moved away from the Dirac point into the valence band as compared to the initial position of E_{F1}. This significantly enhanced the conductivity of graphene, thus the effective conductivity continued to increase. The blue curves in Fig. 2(a) clearly illustrate that the LC resonance gradually weakened as the graphene sheet

became more metallic (from 0 to -5 V) and nearly disappeared at ~-5 V. The LC resonance disappeared due to shorted capacitive gaps of the SRRs.

3.5 Characterization under different photoexcitation power

The terahertz transmission through the graphene-silicon hybrid metasurface under different photoexcitation power of 140 and 420 mW was also measured, as shown in Fig. 4(a) and (b). Amplitude transmissions with different sets of voltages are shown in order to clearly present the modulation trend and the maximum modulation range, since different modulation depths were observed at the same voltage bias when the photoexcitation power was changed. At 140 mW, a lower bias voltage (~0.8 V) was able to achieve the lowest conductivity $\tilde{\sigma}_{eff}(\omega)$ and consequently the strongest LC resonance compared to that under 280 mW excitation. This implied that the initial Fermi energy E_{F2} was closer to the Dirac point than E_{F1}. On the contrary, with high pump power 420 mW, a higher bias voltage (~1.5 V) was required to shift the Fermi energy (E_{F3}) to the Dirac point. Fig. 4(c) illustrates the voltage dependent transmission amplitude of the graphene-silicon hybrid metamaterial without any optical illumination. The absence of any significant modulation confirmed our hypothesis of carrier diffusion from silicon into graphene. The curves in Fig. 4(d) display the terahertz transmission under various pump power with a fixed gate bias voltage at -5 V. We observed a sharp decrease in transmission, from 0.49 to 0.11 at the LC resonance since the original Fermi level of graphene was farther away from the Dirac point as the photoexcitation power was enhanced. It is noted that although the

modulation depth of the hybrid metamaterial was not further enhanced compared to the unpatterned GOS, the active graphene metasurface would indeed promise applications of graphene-based, high-performance integrated photonic devices functioning at defined resonance frequencies. Furthermore, the modulation depth of the hybrid device could be noticeably improved by use of uniquely designed metasurface integrated with a graphene monolayer.

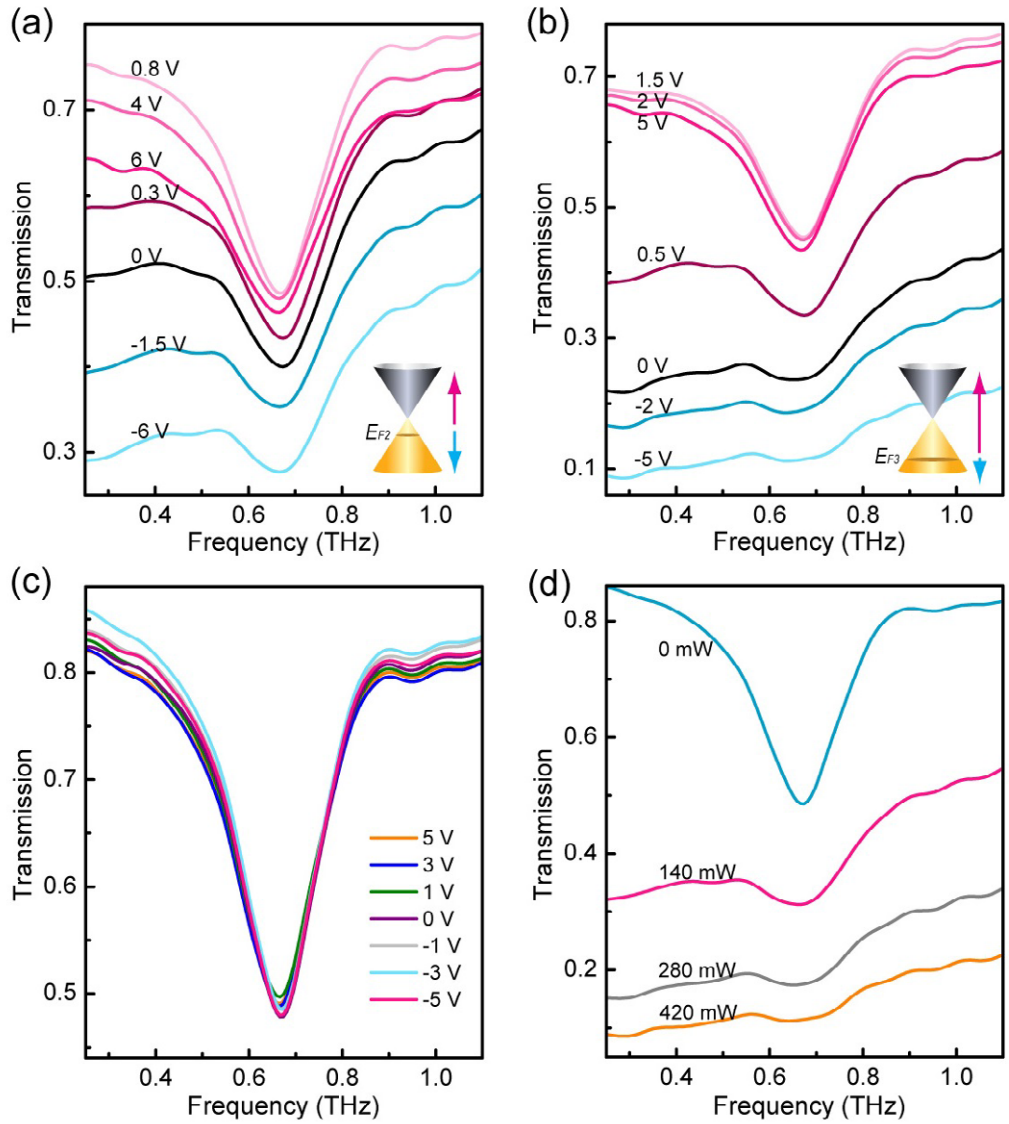

Fig. 4 - (a)-(c) Measured transmission amplitude of the graphene-silicon hybrid metamaterial device as a function of frequency at various gate biases under 532 nm-light illumination powered at 140, 420 and 0 mW, respectively. Insets of (a) and (b): Schematic diagrams of the Fermi level, corresponding to (a), (b), respectively. (d) Spectra of the tunable graphene-silicon hybrid metamaterial modulator biased at -5 V. The resonance strength can be tuned by varying the power of optical excitation.

4. Conclusion

In conclusion, we experimentally demonstrate a highly efficient graphene-silicon hybrid metasurface device that achieved giant modulation of terahertz waves when subjected to a combined stimulus of low gate bias voltage and continuous wave optical illumination. Compared to existing electrically tuned graphene based devices, our design delivers a modulation depth of more than 60% at considerably lower gate voltage (~1 V). Standard thin-film approximation was employed to analyze the mechanism of the tunable transmission behavior. With a higher power of CW photoexcitation, increased number of generated carriers diffused into the graphene layer from the silicon substrate that served as a rich source of free carriers. The LC resonance of the graphene-silicon metamaterial weakened as the effective conductivity of the graphene and photodoped silicon layer increased. Active metamaterials made from integrated graphene monolayer and conventional silicon substrate implemented here has the potential to transform the electronic and photonic

landscape, thus would certainly lead to high-performance real world photonic devices compatible with the state of the art silicon based technology.

Acknowledgements

This work was supported by the U.S. National Science Foundation (Grand No. ECCS-1232081), the National Key Basic Research Special Foundation of China (Grant No. 2014CB339800), the National Science Foundation of China (Grant Nos. 61138001, 61107085, 61107053, 61422509 and 61427814), the Program for Changjiang Scholars and Innovative Research Team in University (Grant No. IRT13033), and the Major National Development Project of Scientific Instruments and Equipment (Grant No. 2011YQ150021).

Appendix A. Supplementary data

Supplementary data associated with this article can be found, in the online version.

References

[1] Valentine J, Li J, Zentgraf T, Bartal G, Zhang X. An optical cloak made of dielectrics. Nat Mater 2009; 8:568-71.

[2] Pendry JB. Negative Refraction Makes a Perfect Lens. Phys Rev Lett 2000; 85:3966-9.

[3] Kabashin AV, Evans P, Pastkovsky S, Hendren W, Wurtz GA, Atkinson R, et al. Plasmonic nanorod metamaterials for biosensing. Nat Mater 2009; 8:867-71.

[4] Chen H-T, Padilla WJ, Zide JMO, Gossard AC, Taylor AJ, Averitt RD. Active

terahertz metamaterial devices. Nature 2006; 444:597-60.

[5] Lee SH, Choi M, Kim T-T, Lee S, Liu M, Yin X, et al. Switching terahertz waves with gate-controlled active graphene metamaterials. Nat Mater 2012; 11:936-41.

[6] Mousavi SH, Kholmanov I, Alici KB, Purtseladze D, Arju N, Tatar K, et al. Inductive tuning of fano-resonant metasurfaces using plasmonic response of graphene in the mid-infrared. Nano Lett 2013; 13:1111-7.

[7] Valmorra F, Scalari G, Maissen C, Fu W, Scho nenberger C, Choi JW, et al. Low-bias active control of terahertz waves by coupling large-area CVD graphene to a terahertz metamaterial. Nano Lett 2013; 13:3193-8.

[8] Piper JR, Fan S. Total absorption in a graphene monolayer in the optical regime by critical coupling with a photonic crystal guided resonance. ACS Photonics 2014; 1:347-53.

[9] Degl'Innocenti R, Jessop DS, Shah YD, Sibik J, Zeitler A, Kidambi PR, et al. Low-bias terahertz amplitude modulator based on split-ring resonators and graphene. ACS Nano 2014; 8:2548-54.

[10] Dolling G, Enkrich C, Wegener M, Soukoulis CM, Linden S. Low-loss negative-index metamaterial at telecommunication wavelengths. Opt Lett 2006; 31:1800-2.

[11] Gupta S, Caloz C. Analog signal processing in transmission line metamaterial structures. Radioengineering 2009; 18:155-67.

[12] Paul O, Beigang R, Rahm M. Highly selective terahertz bandpass filters based on trapped mode excitation. Opt Express 2009; 17:18590-5.

[13] Shrekenhamer D, Rout S, Strikwerda AC, Bingham C, Averitt RD, Sonkusale S, et al. High speed terahertz modulation from metamaterials with embedded high

electron mobility transistors. Opt Express 2011; 19:9968-75.

[14] Singh R, Xiong J, Azad AK, Yang H, Trugman SA, Jia QX, et al. Optical tuning and ultrafast dynamics of high-temperature superconducting terahertz metamaterials. Nanophotonics 2012; 1:117-23.

[15] Padilla WJ, Taylor AJ, Highstrete C, Lee M, Averitt RD. Dynamical electric and magnetic metamaterial response at terahertz frequencies. Phys Rev Lett 2006; 96:107401.

[16] Chen P-Y, Alù A. Atomically thin surface cloak using graphene monolayers. ACS Nano 2011; 5:5855-63.

[17] Zhou F, Bao Y, Cao W, Stuart CT, Gu J, Zhang W, et al. Hiding a realistic object using a broadband terahertz invisibility cloak. Sci Rep 2011; 1:78.

[18] Liang D, Gu J, Han J, Yang Y, Zhang S, Zhang W. Robust large dimension terahertz cloaking. Adv Mater 2012; 24:916-21.

[19] Yan R, Sensale-Rodriguez B, Liu L, Jena D, Xing HG. A new class of electrically tunable metamaterial terahertz modulators. Opt Express 2012; 20:28664-71.

[20] Baron CA, Elezzabi AY. A magnetically active terahertz plasmonic artificial material. Appl Phys Lett 2009; 94:071115.

[21] Gu J, Singh R, Liu X, Zhang X, Ma Y, Zhang S, et al. Active control of electromagnetically induced transparency analogue in terahertz metamaterials. Nat Commun 2012; 3:1151.

[22] Fan K, Strikwerda AC, Zhang X, Averitt RD. Three-dimensional broadband tunable terahertz metamaterials. Phys Rev B 2013; 87:161104.

[23] Wen Q-Y, Tian W, Mao Q, Chen Z, Liu W-W, Yang Q-H, et al. Graphene based all-optical spatial terahertz modulator. Sci Rep 2014; 4:7409.

[24] Novoselov KS, Geim AK, Morozov SV, Jiang D, Zhang Y, Dubonos SV, et al. Electric field effect in atomically thin carbon films. Science 2004; 306:666-9.

[25] Maeng I, Lim S, Chae SJ, Lee YH, Choi H, Son J-H. Gate-controlled nonlinear conductivity of Dirac fermion in graphene field-effect transistors measured by terahertz time-domain spectroscopy. Nano Lett 2012; 12:551-5.

[26] V. G. Kravets, F. Schedin, R. Jalil, L. Britnell, K. S. Nomoselov, A. N. Grigorenko. Surface hydrogenation and optics of a graphene sheet transferred onto a plasmonic nanoarray. J Phys Chem C 2012; 116:3882-7.

[27] Sensale-Rodriguez B, Yan R, Kelly MM, Fang T, Tahy K, Hwang WS, et al. Broadband graphene terahertz modulators enabled by intraband transitions. Nat Commun 2012; 3:780.

[28] Jnawali G, Rao Y, Yan H, Heinz TF. Observation of a transient decrease in terahertz conductivity of single-layer graphene induced by ultrafast optical excitation. Nano Lett 2013; 13:524-30.

[29] Ryzhii V, Ryzhii M, Otsuji T. Negative dynamic conductivity of graphene with optical pumping. J Appl Phys 2007; 101:083114.

[30] Li J, Zhou Y, Quan B, Pan X, Xu X, Ren Z et al. Graphene-metamaterial hybridization for enhanced terahertz response. Carbon 2014; 78: 102-12.

[31] Ju L, Geng B, Horng J, Girit C, Martin M, Hao Z, et al. Graphene plasmonics for tunable terahertz metamaterials. Nat Nanotechnol 2011; 6:630-4.

[32] Sensale-Rodriguez B, Yan R, Rafique S, Zhu M, Li W, Liang X, et al. Extraordinary control of terahertz beam reflectance in graphene electro-absorption modulators. Nano Lett 2012; 12:4518-22.

[33] Singh R, Smirnova E, Taylor AJ, O'Hara JF, Zhang W. Optically thin terahertz metamaterials. Opt Express 2008; 16:6537-43.

[34] Yen TJ, Padilla WJ, Fang N, Vier DC, Smith DR, Pendry JB, et al. Terahertz magnetic response from artificial materials. Science 2004; 303: 1494-6.

[35] Azad AK, Dai J, Zhang W. Transmission properties of terahertz pulses through subwavelength double split-ring resonators. Opt Lett 2006; 31: 634-6.

[36] Li X, Cai W, An J, Kim S, Nah J, Yang D, et al. Large-area synthesis of high-quality and uniform graphene films on copper foils. Science 2009; 324:1312-4.

[37] Wu B, Geng D, Guo Y, Huang L, Xue Y, Zheng J, et al. Equiangular hexagon-shape-controlled synthesis of graphene on copper surface. Adv Mater 2011; 23:3522-5.

[38] Li X, Zhu Y, Cai W, Borysiak M, Han B, Chen D, et al. Transfer of large-area graphene films for high-performance transparent conductive electrodes. Nano Lett 2009; 9:4359-63.

[39] Grischkowsky D, Keiding S, Exter M, Fattinger Ch. Far-infrared time-domain spectroscopy with terahertz beams of dielectrics and semiconductors. J Opt Soc Am B 1990; 7:2006-15.

[40] Linden S, Enkrich C, Wegener M, Zhou J, Koschny T, Soukoulis CM. Magnetic response of metamaterials at 100 terahertz. Science 2004; 306: 1351-3.

[41] Ren L, Zhang Q, Yao J, Sun Z, Kaneko R, Yan Z, et al. Terahertz and infrared spectroscopy of gated large-area graphene. Nano Lett 2012;12: 3711-5.

[42] Takii E, Eto T, Kurobe K, Shibahara K. Ultra-shallow junction formation by green-laser annealing with light absorber. Jpn J Appl Phys 2005; **44:**L756-9.

[43] Zhang W, Azad AK, Han J, Xu J, Chen J, Zhang X-C. Direct observation of a transition of a surface plasmon resonance from a photonic crystal effect. Phys Rev Lett 2007; 98:183901.

[44] Weis P, Garcia-Pomar JL, Höh M, Reinhard B, Brodyanski A, Rahm M. Spectrally wide-band terahertz wave modulator based on optically tuned graphene. ACS Nano 2012; 6:9118-24.

[45] Yan H, Li X, Chandra B, Tulevski G, Wu Y, Freitag M, et al. Tunable infrared plasmonic devices using graphene/insulator stacks. Nat Nanotechnol 2012; 7:330-4.

[46] Davoyan AR, Morozov MY, Popov VV, Satou A, Otsuji T. Graphene surface emitting terahertz laser: diffusion pumping concept. Appl Phys Lett 2013; 103: 251102.